# Dynamics of solvation in supercooled liquids confined to the pores of sol-gel glasses

C. Streck, Yu. B. Mel'nichenko,* and R. Richert
*Max-Planck-Institut für Polymerforschung, Ackermannweg 10, D-55128 Mainz, Germany*
(Received 21 September 1995)

We have measured the solvation dynamics of the probe molecule quinoxaline in a glass-forming solvent, 2-methyltetrahydrofuran, geometrically confined to the pores of sol-gel glasses having nominal pore diameters $\phi$=2.5, 5.0, and 7.5 nm. Within the time range 1 ms$\leqslant t \leqslant$1 s the $\alpha$ process and a second extremely slow process are observed. On the basis of emission spectra, the latter relaxation is assigned to a surface layer with strongly frustrated dynamics, opposed to the picture of a certain fraction of pores entirely filled with liquid of reduced molecular mobility. According to the Stokes-shift results for porous samples, the thickness of this surface layer increases significantly with $T_g \leftarrow T$ for the system under study. The results are compared with solvation dynamic experiments for the bulk solvent and with dielectric relaxation measurements.

## I. INTRODUCTION

It is well established that the dynamics of liquids are strongly affected by the immediate presence of a solid surface.[1–8] By physical and/or chemical interactions, a solid interface tends to induce anisotropic molecular alignments and oscillatory density fluctuations with a concomitant striking impact on the molecular dynamics in the surface layer of the liquid, which is typically several molecular diameters in thickness.[8] The extent of such effects depend strongly on the liquid under study and on the chemical and physical properties of the interface, so that no generally valid rule regarding confinement effects can be established easily. Therefore, despite the currently growing interest in the effects of geometrical confinement, only little is known on the detailed mechanisms with which confinement acts on molecular relaxation processes. Especially for experimental techniques which are not surface specific, it is crucial that very large surface to volume ratios can be obtained for porous glasses, which renders these systems interesting to both fundamental science and technical applications.[9,10]

The effects of geometrical confinement are of special interest for liquids which are capable of supercooling. In such materials, decreasing the temperature to well below the melting point preserves the disordered liquidlike structure, but leads to a marked increase of the molecular relaxation times.[7,11,12] Further cooling eventually leads to nonergodic systems at the glass transition temperature $T_g$, where the time scale of the structural $\alpha$ relaxation tends to exceed the time window of the experiment, say 100 s.[13] The pronounced increase in relaxation times as $T_g \leftarrow T$ is believed to be paralleled by an enhancement of cooperativity of molecular motions. The spatial scales $\xi$ on which cooperativity is effective are assumed to attain values around $\xi \approx 1$–3 nm at $T = T_g$.[14] In this case, the range of cooperativity may compte with the pore size for a supercooled liquid confined to the mesopheres of a porous glass.

The technique of solvation dynamics as used here employs chromophores as probe molecules at low concentrations, whose emission spectrum is monitored as a function of time following its electronic excitation.[15–18] Provided that the dipole moment in the excited state ($\mu_E$) differs substantially from that in the ground state ($\mu_G$), electronic excitation induces a dielectric relaxation process in the immediate vicinity of the chromophore, which can be observed in terms of a time-dependent red shift of the mean emission energy $\nu$ of the probe molecule. For the long time scales of molecular relaxation usually found in supercooled liquids close to their glass transition temperature $T_g$, phosphorescent probes are used with correspondingly long excited state lifetimes $\tau_{ph}$.[18–20] Solvation dynamics experiments in bulk liquids have revealed that the temporal evolution of the Stokes shift closely reflects the dielectric relaxation behavior $\varepsilon^*(\omega)$ of the solvent.[20–22] The optical technique is, however, sensitive only to the features within a small number of solvation layers, i.e., solvation dynamics probe the local dielectric properties in the vicinity of the chromophore.[23] In this context, measurements of the Stokes shift $\Delta\nu$ as a function of pore size are highly desirable, because they should lead to an estimate of the spatial range of interactions between a chromophore and the solvent. Within the geometrical confinement of a porous glass, a particular chromophore will thus sense predominantly the dynamics of the pore it resides in. Consequently, solvation dynamics results are not expected to be affected by Maxwell-Wagner polarization, which appears as a relaxation peak in dielectric relaxation spectroscopy of heterogeneous systems,[24] e.g., for a slightly conducting liquid within an insulating glass.[25]

In the present study, we investigate the effect of confinement on molecular dynamics of a supercooled liquid by solvation dynamics spectroscopy. Evidence is found for the existence of a surface layer at the pore walls with strongly hindered orientational mobility and with a significant dependence of its thickness on temperature. The remaining inner pore liquid displays a relaxation process reminiscent of the bulk $\alpha$ or structural relaxation down to pore diameters of 2.5 nm, but associated with faster response times and lowered apparent activation energies as the pore size decreases. This optical technique of probing the time dependence of orientational dielectric polarizability yields complimentary information with respect to dielectric relaxation spectroscopy, because (i) it is insensitive to Maxwell-Wagner polarization

 

effects, which complicate the assignment of loss peaks, and (ii) it is capable of assigning the extremely slow process to immobilized liquid portions in each pore, opposed to the picture of some pores exhibiting completely frozen dynamics, while the entire liquid in other pores is relaxing. Additionally, the results demonstrate directly the very limited spatial range relevant for the solvation free energy of a dipolar chromophore embedded in a polar environment, thereby emphasizing that solvation dynamics can be employed for locally probing dielectric relaxation phenomena.

## II. EXPERIMENTAL

The glass-forming liquid 2-methyltetrahydrofuran (MTHF) obtained from Aldrich was distilled and passed through $Al_2O_3$ filters to remove polar contaminations directly before filling the pores. Quinoxaline (QX) obtained from Aldrich was distilled and sublimated and then dissolved in MTHF at a concentration of $\approx 10^{-4}$ mol/mol. Due to these low QX concentrations the probability of finding two QX molecules in one pore is practically zero. As porous glasses with sufficiently high optical quality we used Gelsil glasses of cylindrical shape (10 mm $\phi$, 5 mm thick) being produced by sol-gel technology[10] and purchased from GelTech. The nominal pore diameters are $\phi = 2.5$, 5.0, and 7.5 nm. According to a Brunauer-Emmett-Teller analysis supplied by GelTech, the actual data in the above order of $\phi$ are: pore diameters 2.6, 4.6, and 8.4 nm; pore volume fractions 0.39, 0.68, and 0.72; and surface areas 609, 594, and 342 $m^2/g$. In order to obtain clean pore surfaces, the glass was heated in vacuum to 400 °C for 24 h. The glasses were filled with QX/MTHF under dry $N_2$ atmosphere and placed into a vacuum sealed sample holder, where it is gently pressed in contact to a sapphire window. The remaining volume within the sample holder was also filled with the QX/MTHF liquid to ensure complete liquid content in the pores for the entire experiment and to improve thermal contact to the brass walls. This sample housing was mounted to the cold stage of a closed cycle He refrigerator (Leybold, RDK 10-320, RW2) and temperature stability within $\pm 50$ mK was achieved by a temperature controller (Lake Shore, LS 330) equipped with calibrated diode sensors. Samples were allowed to equilibrate for at least one hour at each set temperature prior to a measurement. Subsequent measurements for a sample were done from high to low temperatures.

As an excitation source we employed an excimer laser (Radiant Dyes, RD-EXC-100) operated at 308 nm with pulse width $\approx 25$ ns, pulse energy 120 mJ, and at a repetition rate of 1 Hz. The attenuated ($\div 10$) laser beam was passed through a filter (Schott, DUG-11) to block any components in the visible wavelength range. The aperture was limited such that excitation outside the porous glass cylinder is avoided. The phosphorescence from QX was coupled via fiber optics to a triple grating monochromator (EG&G, 1235) and registered by a micro-channel-plate intensified diode array camera (EG&G, 1455B-700-HQ) with controller (EG&G, 1471 A), gating options (EG&G, 1304), and synchronization facilities (EG&G, 9650). The spectra, consisting of 730 channels with a resolution of 0.04 nm/channel for the 1800 g/mm holographic grating, were wavelength calibrated with Xe and Kr calibration lamps. The time resolution is defined either by gating the camera with gate widths between 100 ns and 10 ms or by successive readouts of the controller at a speed of up to 50 spectra/s. For the probe molecule QX the usable time range is lifetime limited ($\tau_{ph} \approx 0.33$ s) to 1 ms$\leq t \leq 1$ s for experiments using porous glasses.

Every one of the $\approx 1600$ spectra obtained in the above manner was subject to a Gaussian fit regarding the electronic $S_0 \leftarrow T_1$ (0-0) transition of QX which reduces the data to the relevant values of the mean emission energy $\nu(t,T)$ and Gaussian width $\sigma$. Typical such spectra of QX/MTHF have been reported elsewhere.[18,20] The luminescence intensity $I(\nu,t,T)$ relates simply to the phosphorescence lifetime in terms of $\int I(\nu,t,T)\, d\nu \propto \exp(-t,\tau_{ph})$ and is thus not evaluated further. For focusing on the Stokes-shift dynamics it is convenient to normalize the $\nu(t)$ data to the so-called Stokes-shift correlation function $C(t)$:[17]

$$C(t) = \frac{\nu(t) - \nu(\infty)}{\nu(0) - \nu(\infty)}. \tag{1}$$

## III. RESULTS

The reason for particularly selecting the QX/MTHF system for the present study of solvation dynamics in geometrical confinement is that bulk MTHF has been investigated in detail in the extremely broad time range covering $10^{-10}$–$10^{2}$ s regarding both solvation dynamics and dielectric relaxation.[22] For the sake of reliability we have repeated the bulk solvation measurements for QX/MTHF under the same experimental conditions and calibrations used for the porous glasses, but with some extension towards lower temperatures relative to previous data. At temperatures sufficiently below the glass transition of MTHF at $T_g \approx 91$ K,[21,26] i.e., in the range 70–85 K, the mean emission energy of QX is time invariant at $\nu(0) = 21\,375$ $cm^{-1}$. Above $T_g$ again a constant value is found in the range 93–100 K but at $\nu(\infty) = 21\,115$ $cm^{-1}$. At intermediate temperatures we find a time-dependent $\nu(t)$, with total Stokes shift $\Delta\nu = \nu(0) - \nu(\infty) = 260$ $cm^{-1}$, being the signature of the dielectrically active $\alpha$ process in MTHF.[21,22] The limiting values $\nu(0) = \nu(t)$ for $T < T_g$ and $\nu(\infty) = \nu(t)$ for $T > T_g$ are independent of $t$ if varied in the range 1 ms$\leq t \leq 1$ s and are thus used to normalize $\nu(t)$ according to Eq. (1). The resulting $C(t)$ data for the bulk sample is well approximated by a Kohlrausch-Williams-Watts[27] (KWW) or stretched exponential law of the form

$$C(t) = \exp[-(t/\tau)^{\beta}], \tag{2}$$

with an exponent $\beta \approx 0.45$.

For the emission energies of QX/MTHF in pores for 70 K$\leq T \leq$100 K we find values in the range 21 100 $cm^{-1} \leq \nu(t,T) \leq 21\,375$ $cm^{-1}$, i.e., the total Stokes shift $\Delta\nu$ is practically not affected by geometrical confinement. The striking impact of the confinement to pores is observed when focusing on the Stokes-shift dynamics $C(t)$ for temperatures 85 K$\leq T \leq$95 K. Experimental $C(t)$ data for bulk and porous samples are depicted in Fig. 1 for $T \approx 92$ K. Without further data analysis it is seen from these $C(t)$ curves that with decreasing pore size $\phi$ the decay separates into an $\alpha$ process which is faster than the bulk $\alpha$ relaxation and a second pro-

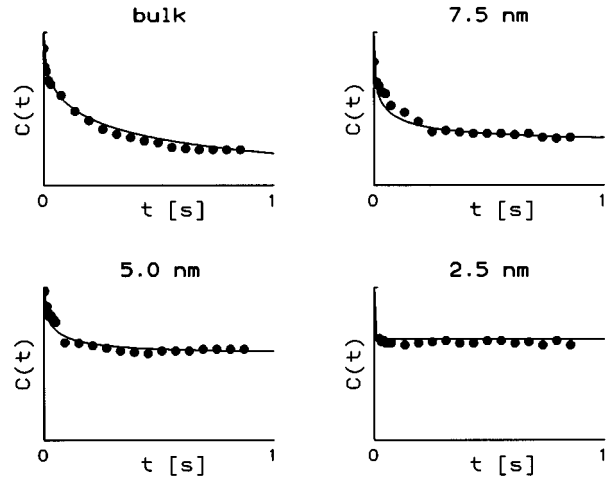


FIG. 1. Experimental results (●) for the normalized decay $C(t)$ of the average $S_0 \leftarrow T_1$ (0-0) emission energy of QX in MTHF at $T \approx 92$ K for bulk and porous samples. The solid lines are reconstructions based on a global fit to all $C(t)$ using Eqs. (3)–(5) and the data in Table I. The linear scales cover the ranges $0 \leqslant C(t) \leqslant 1$ ($\Delta\nu = 260$ cm$^{-1}$) and $0 \leqslant t \leqslant 1$ s in all four panels.

cess with an unresolved slow time constant. For the 2.5 nm pores, only a temperature-dependent change in the relative contributions of fast and slow process is observed. In this case we can only estimate that the fast process is related to $\langle\tau\rangle < 3$ ms and the slow one to $\langle\tau\rangle > 30$ s. In order to quantify these effects as a function of temperature and pore size, we assume a sum of two KWW decays. Since it is obvious that one of the contributions is related to a value of $\tau \gg 1$ s which cannot be resolved within the experimental time window, we fit the data in terms of the sum of a KWW decay and an offset $C_o$:

$$C(t) \approx C_o + (1 - C_o)\exp[-(t/\tau)^{\beta}]. \tag{3}$$

For each of the four pores sizes $\phi$ (bulk is considered $\phi = \infty$) we have recorded $C(t)$ decays at eight different temperatures, so that fits according to the three parameter function in Eq. (3) yield $4 \times 8 \times 3 = 96$ values for $C_o(\phi,T)$, $\tau(\phi,T)$, and $\beta(\phi,T)$. An inspection of these results unambiguously indicates that (i) a decreasing pore size $\phi$ leads to an increase in $C_o$ at $T > T_g$ and to a decrease of the apparent activation energy of $\tau(T)$, (ii) lowering the temperature results in a sigmoidal shaped increase of $C_o$ for $\phi < \infty$ [for the bulk sample $C_o(\infty,T) = 0$], with the onset temperature of this effect being shifted to higher $T$ as $\phi$ is lowered, (iii) $\tau(\phi < \infty,T) < \tau(\phi = \infty,T)$, and (iv) $\beta(\phi < \infty) < \beta(\phi = \infty)$, with approximately $\beta \neq \beta(T)$. In order to better extract the information regarding the impact of $\phi$ and $T$ on the decay behavior of $C(t)$, we have conducted a global fit to the 32 $C(t)$ curves under the following parameter restrictions: For the stretched exponent $\beta$ temperature invariant values $\beta(\phi = \infty) = 0.40$ and $\beta(\phi < \infty) = 0.35$ are used. Since the range of temperatures is too small the actual curvature in an activation plot of $\tau(T)$,[22] the temperature dependence of $\tau$ is modeled by an Arrhenius law,

$$\tau = \tau_0(\phi)\exp[E_a(\phi)/kT]. \tag{4}$$

TABLE I. Results of the global fit to all $C(t)$ data for the bulk and porous samples. $E_a$ and $\tau_0$ are used in Eq. (4) to define the decay time constant $\tau(\Phi,T)$. $T_\sigma$ and $\Theta$ are used in Eq. (5) to define the offset $C_o(\phi,T)$. For $\phi = 2.5$ nm the values of $\tau(T)$ are beyond experimental resolution.

| Sample | $E_a$/kJ mol$^{-1}$ | $-\log_{10}(\tau_0/\text{s})$ | $T_\sigma$/K | $\theta$ |
|---|---|---|---|---|
| Bulk | 110 | 62.9 | | 0.00 |
| 7.5 nm | 75 | 44.0 | 90.8 | 0.06 |
| 5.0 nm | 65 | 38.7 | 92.1 | 0.15 |
| 2.5 nm | | | 93.5 | 0.20 |

The sigmoidal-like change of $C_o$ with $T$ is represented by an arctan($T$) function with high-temperature offset $\Theta$ in the form

$$C_0 = \Theta(\phi) + [1 - \Theta(\phi)](\tfrac{1}{2} - \pi^{-1}\ \arctan\{0.8\ \text{K}^{-1}[T - T_\sigma(\phi)]\}). \tag{5}$$

In this function $C_o(T \to 0) = 1$, $C_o(T \to \infty) = \Theta$ the constant 0.8 K$^{-1}$ defines a $\phi$-independent slope of $C_o(T)$ at $T = T_\sigma$, and $T_\sigma$ positions the inflection point of $C_o(T)$ on the temperature scale. For the bulk sample we set $C_o(\phi = \infty,T) \equiv 0$. The results of a simultaneous fit to all $C(t)$ data under the above parameter limitations are compiled as $\tau_0(\phi)$, $E_a(\phi)$, $\Theta(\phi)$, and $T_\sigma(\phi)$ in Table I. The resulting functions $C_o(\phi,T)$ and $\tau(\phi,T)$ are shown for the range 80 K$\leqslant T \leqslant$100 K in Figs. 2 and 3, respectively. We can now reconstruct the $C(t)$ decays along the lines of Eqs. (3)–(5) using the parameters of Table I. Such fits are included as lines in Fig. 1, whereas, the symbols represent the experimental data for $T \approx 92$ K for the four different samples.

## IV. DISCUSSION

In order to visualize how temperature and pore size affect the dynamics of the liquid, Fig. 4 presents a series of reconstructed decays parametric in pore size $\phi$ and temperature $T$. The panel related to the bulk liquid shows the $\alpha$ process of the solvent in terms of $C(t)$, with no signature for a further,

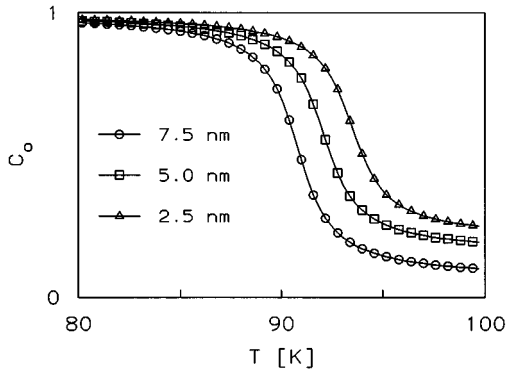


FIG. 2. Fit parameter $C_o$ used in Eq. (3), calculated from Eq. (5) with the parameters listed in Table I. For the bulk sample $C_o \equiv 0$ is temperature invariant. The plot demonstrates that both parameters of Eq. (5), $T_\sigma$ and $\Theta$, increase if the pore size $\phi$ is varied in the following order: 7.5 nm (○), 5.0 nm (□), 2.5 nm (△).

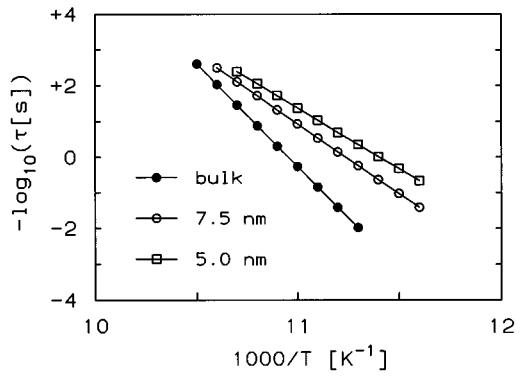


FIG. 3. Fit parameter $\tau$ used in Eq. (3), calculated from Eq. (4) with the parameters listed in Table I. For the 2.5 nm porous sample $\tau$ is below the experimental limit of resolution. The plot demonstrates that the apparent activation energy $E_a$ used in Eq. (4) decreases if the pore size $\phi$ is varied in the following order: bulk (●), 7.5 nm (○), 5.02 nm (□).

faster or slower, dielectrically active relaxation process. A previous[21] analysis of these data within the framework of the dynamical mean spherical approximation (MSA) has indicated that $C(t)$ for bulk QX/MTHF complies with a dielectric relaxation of pure MTHF according to the empirical Cole-Davidson (CD)[28] function in the frequency domain, which reads $\varepsilon^*(\omega)=\varepsilon_\infty+\Delta\varepsilon(1+i\omega\tau_{\mathrm{CD}})^{-\gamma_{\mathrm{CD}}}$, with $\gamma_{\mathrm{CD}}\approx 0.5$. The corresponding Stokes shift of $\Delta\nu=260\ \mathrm{cm}^{-1}$ for QX in bulk MTHF is in accord with the dielectric relaxation strength of MTHF, $\Delta\varepsilon=18$ at $T\approx T_g$.[29] The present observation of $\Delta\nu$ being practically unaffected by geometrical confinement down to pore diameters of 2.5 nm yields direct evidence for the chromophore serving as a highly local probe for the dielectric properties, since the relevant length scale

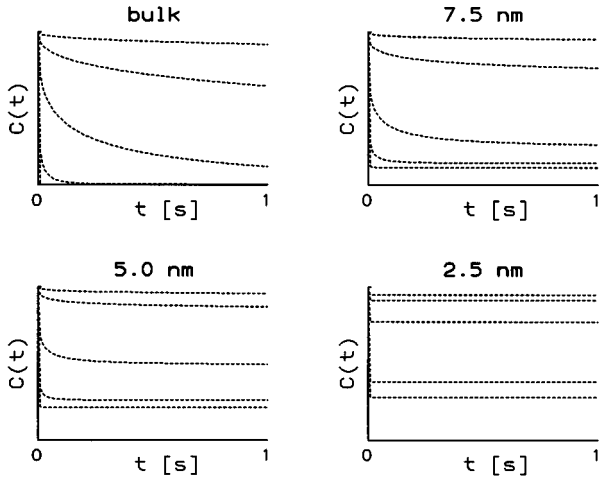


FIG. 4. Reconstructed normalized decays $C(t)$ for the average $S_0\leftarrow T_1$ (0-0) emission energy of QX in MTHF for bulk and porous samples, as indicated. The dashed lines are based on a global fit to all $C(t)$ using Eqs. (3)–(5) and the data in Table I. For each pore size $C(t)$ is shown for the temperatures 87.5, 90.0, 92.5, 95.0, and 97.5 K, in the order from upper to lower curves. The linear scales cover the ranges $0\leqslant C(t)\leqslant 1$ ($\Delta\nu=260\ \mathrm{cm}^{-1}$) and $0\leqslant t\leqslant 1$ s in all four panels.

related to the solvation free energy cannot exceed the pore size significantly. Otherwise, the Stokes shift $\Delta\nu$ would have been decreased to $\sim\kappa\Delta\nu$, where $\kappa$ is the porosity of the sample delineating the volume fraction of the pores, because in the glass volume fraction, $1-\kappa$, no orientational relaxation is active. In accord with this result, it can be estimated that for the solvation free energy of spherical point dipoles in polar solvents mainly the first solvent shell is relevant.[23]

In the porous systems, we find the dielectric $\alpha$ process which is faster than the equivalent relaxation in the bulk as indicated in Fig. 3. The decrease of $\beta$ in Eq. (3) relative to the value for the bulk liquid reflects a broadening of the underlying relaxation time distribution, which in all cases deviates strongly from exponential ($\beta=1$) response functions. These two features regarding the $\alpha$ process, acceleration, and broadening, in the case of geometrical confinement are identically observed by dielectric spectroscopy on pure liquids in mesopores.[25,30–32] Additionally, we have direct evidence for the $\alpha$-relaxation strength $\Delta\varepsilon_\alpha$ being suppressed by either lowering the pore size or decreasing the temperature. Within the $C(t)$ data, a measure for this value $\Delta\varepsilon_\alpha$ is $(1-C_o)$, where $C_o$ is the offset in Eq. (3), whose dependence on $\phi$ and $T$ is shown in Fig. 2. The most natural basis for such a variation of $\Delta\varepsilon_\alpha$ is the assumption of the number of molecules participating in the $\alpha$ relaxation being $\phi$ and $T$ dependent. In general, other parameters which affect $\Delta\varepsilon$ are the effective dipole moment $\mu_{\mathrm{eff}}$ or $g^{1/2}\mu$ and absolute temperature $T$.[24] However, the trivial variation of $\Delta\varepsilon$ with temperature by virtue of its $\mu^2/3$ kT dependence is negligible in the present small temperature range. Secondly, it has been shown previously for bulk MTHF that the effective dipole moment $\mu_{\mathrm{eff}}$ is temperature invariant in the vicinity of $T_g$.[33]

A nontrivial problem related to the observed reduction of the $\alpha$-relaxation strength is to discriminate between the following two possibilities behind lowering the number of molecules participating in the $\alpha$ process. One is that for a certain number of pores the entire liquid within these pores is frozen, the other possibility is assuming that simultaneously in all pores a certain fraction of the liquid is immobilized. In the former case, an ensemble averaged incomplete solvation process is seen, because some of the pores display the total solvation energy $\Delta\nu=260\ \mathrm{cm}^{-1}$ [a Stokes shift from $\nu(0)=21\,375\ \mathrm{cm}^{-1}$ to $\nu(\infty)=21\,115\ \mathrm{cm}^{-1}$], while those with frozen dynamics will yield a time-independent emission at $\nu(0)=21\,375\ \mathrm{cm}^{-1}$. In the latter case, the orientational polarizability around each probe molecule is reduced by immobilization, such that all pores identically display a smaller total solvation energy related to a shift from $\nu(0)=21\,375\ \mathrm{cm}^{-1}$ to a value $\nu>\nu(\infty)$. Since we have measured not only $\nu(t)$ but the entire $S_0\leftarrow T_1$(0-0) spectra as a function of time, the data is capable of discriminating between the two above situations on the basis of the inhomogeneous spectral width $\sigma(t)$. If a mean emission energy (for $t\gg 0$) at $\nu=[\nu(0)+\nu(\infty)]/2$ would originate from equally weighted but distinct emissions at $\nu(0)$ and at $\nu(\infty)$, according to the case of equal numbers of frozen and active pores, then the observed line widths should be at least twice the $\sigma(0)$ [$\approx\sigma(\infty)$], because $\Delta\nu>\sigma(0)$. In the case of partially frozen dynamics in each pore, the observed width is expected to maintain the value $\sigma(0)\approx 190\ \mathrm{cm}^{-1}$. The solvation dynamics results clearly argues against the picture of some pores filled with entirely

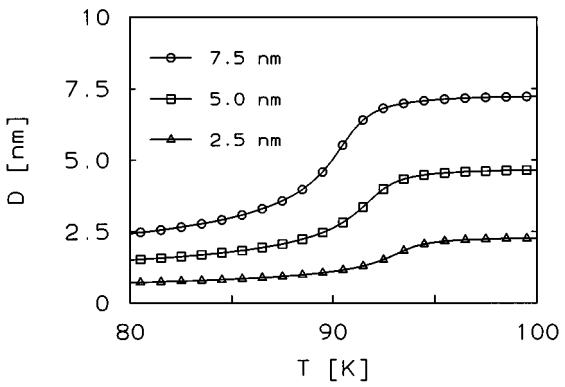


FIG. 5. Effective diameter $D$ of the inner pore liquid as a function of temperature, calculated on the basis of $C_o(\phi,T)$ results and assuming spherical pores, $D=\phi\ [1-C_o(\phi,T)]^{1/3}$. Accordingly, the surface layer thickness $\rho$ decreases as $D$ approaches $\phi$ with increasing temperature. The curves are plotted for the average pore sizes of the samples $\phi$=7.5 nm (○), 5.0 nm (□), and 2.5 nm (△).

frozen liquid and others with dynamically active content, because the width does not exceed $\sigma(0)$ by more than 5% for all $C(t)$ curves. We therefore adopt the picture of relating the decrease of $\Delta\varepsilon_\alpha\sim(1-C_o)$ to an enhanced fraction of immobilized liquid in each pore.

Following the above and previous[25,30–32] evidence derived from dielectric relaxation data, we assign the slow process (which cannot be quantified in terms of its $\tau$ and $\beta$, but only by its strength $C_o$) to the highly frustrated dynamics of molecules within a surface layer in physical and/or chemical contact with the pore walls. The relaxation strength $\Delta\varepsilon_s$ of this surface layer is proportional to $C_o$, and as for $\Delta\varepsilon_\alpha$ we relate $\Delta\varepsilon_s$ to the number of molecules associated with the surface layer. Conservation of particles now requires a constant $\Delta\varepsilon_\alpha+\Delta\varepsilon_s$, in accord with our observation $\Delta\varepsilon_\alpha+\Delta\varepsilon_s=\Delta\varepsilon\neq\Delta\varepsilon(\phi,T)$, corresponding to $\Delta\nu$=260 cm$^{-1}$. This rules out a surface layer relaxation strength much in excess of the bulk $\Delta\varepsilon$ for this system, as seen in other porous glasses via dielectric experiments.[25,31,32] As a consequence, the parameter $C_o$ in Fig. 2 indicates the relative amount of liquid associated with the surface layer of thickness $\rho$ as a function of pore size and temperature. The high-temperature values of $C_o(\phi,T)$, $\Theta(\phi)$, are consistent with a pore size independent surface layer thickness of $\rho$=0.1 ($\pm$0.024) nm, calculated as $\phi/2\{1-[1-\Theta(\phi)]^{1/3}\}$, i.e., assuming spherical pores for simplicity. Since this value is significantly below the thickness of a MTHF monolayer, the average of 0.1 nm is expected to be determined by only those molecules which are chemically trapped at the glass surface even at elevated temperatures, presumably by the silanol groups of the glass surface. The increase of $\rho$ with decreasing temperature results in a decreasing diameter $D$ associated with the remaining inner pore liquid, which again on the basis of $C_o(\phi,T)$ and assuming spherical pores is given by $D=\phi[1-C_0(\phi,T)]^{1/3}$. The resulting $D(T)$ is plotted in Fig. 5, showing that $D$ attains values as low as 2.5 nm at $T\approx$90 K for $\phi$=5.0 nm and at $T\approx$80 K for $\phi$=7.5 nm. Therefore $D(\rho)$ is a substantial effect which may not be disregarded when rationalizing the confinement effect on the inner pore dynamics.

It is an attractive idea to correlate the decrease of the number of molecules participating in the $\alpha$ process as the temperature is lowered with an increasing length scale $\xi$ of cooperativity. One could imagine that a cooperatively rearranging region (CRR) looses relaxation strength as $\xi$ approaches the radius given by the amount of inner pore liquid subject to the $\alpha$ relaxation, because the outer immobile molecules will gradually suppress the relaxation process. Actually, $\xi(T)$ deduced from such a picture should be considered as an effective value, composed of $\xi_\alpha$ and $\xi_s$, which respectively originate from the inner liquid and surface layer, with possibly different values and temperature dependences. The more severe objection against estimating $\xi(T)$ from the surface layer thickness or from $\Delta\varepsilon_\alpha(T)$ is that a value of $\xi$ substantially exceeding intermolecular distances contrasts the highly separated relaxation times related to the molecular dynamics of the inner liquid and of the surface layer, because an approach of the $\alpha$-relaxation time towards the time scale of the surface dynamics should preceed the eventual freezing of relaxation strength. However, such a divergencelike behavior of the $\alpha$-relaxation time towards much longer time scales while $\Delta\varepsilon_\alpha\rightarrow0$ has not been observed. Alternatively, a CRR in the strict sense of Adam and Gibbs,[34] where all constituents of a CRR exhibit identical dynamics, should become frozen entirely when its boundary is in contact with immobile molecules. Within such a picture proposed recently,[30] a gradual decrease of $\Delta\varepsilon_\alpha$ must be associated with a varying fraction of entirely frozen pores regarding their dynamics, in contrast to the observed inhomogeneous linewidths discussed above.

In view of the above notions regarding cooperativity, it is more realistic to simply assume that the surface layer grows in thickness on the expense of the inner pore liquid as the temperature is lowered, with the two phases displaying highly distinct dynamics, i.e., with no gradual transition regarding the relaxation time scales. Such a sharp transition in dynamical behavior is also observed in dielectric relaxation experiments in terms of distinct loss peaks,[25,31,32] rather than a continuous distribution, and in viscosity measurements of ultrathin liquid films,[4] where the viscosity tends to diverge abruptly at a film thickness of several monolayers. However, it remains to be explained why the present average surface layer thickness results $\rho(T)$ display a transition from 0.1 nm to $\phi/2$ at temperatures close to the glass transition $T_g$, i.e., in a narrow temperature range around $T\approx$92 K for MTHF. The relaxation behavior of supercooled liquids near $T_g$ are commonly characterized by extremely long relaxation times $\tau$ combined with a strong sensitivity of $\tau$ to temperature variations. Therefore, at $T_g$ only small additional barriers are needed to completely freeze the dynamics, analogous to finding almost infinitely long relaxation times at temperatures slightly below $T_g$. Since an immobile molecule or solid interface are likely to impose an additional barrier to an adjacent mobile site, it is not surprising that the number of immobilized molecules increases substantially at precisely those temperatures where the molecular mobility of the bulk liquid is highly frustrated. Since the pore surface is rough or even fractal-like for sol-gel-type porous glasses,[2] the transition of $\rho(T)$ from 0.1 nm to $\phi/2$ should be a gradual process as a function of $T$, because roughness results in a distribution of liquid-to-glass interaction energies.

For the time scales $\tau$ of the inner pore liquid's $\alpha$ process,

we find an acceleration of the $\alpha$ relaxation upon lowering the pore size $\phi$, in accord with a confinement-induced shift of $T_g$ towards lower temperatures found for similar liquids in porous glasses.[25,35–38] In the present case, this effect is paralleled by a reduction of the apparent activation energy as seen in Fig. 3. It should be emphasized that the linear behavior in the activation plot Fig. 3 is an approximation to the real $\tau(T)$ curve of MTHF, which displays marked deviations from simple activated behavior in the extended range 90 K$\leqslant T \leqslant$180 K.[22] For a particular temperature, the present results indicate a faster $\alpha$ process if the pore size is lowered. The impact of temperature on the relaxation time of a confined liquid is thus a combination of a bulklike effect and, additionally, the effect of the temperature-dependent effective pore size for the inner liquid, due to the growing surface layer thickness $\rho$ as $T$ decreases. Upon cooling, $\rho(T)$ thus counteracts the increase of $\tau$, thereby leading to a less pronounced variation of $\tau$ with $T$, i.e., to a lower apparent activation energy, as observed in Table I and Fig. 3.

For rationalizing the confinement effects on the $\alpha$-relaxation time, it is important to know whether the inner pore liquid is subject to constant pressure or constant volume conditions, corresponding to the question of the extent by which the liquid is capable of flowing macroscopically within the porous glass in order to establish the ambient pressure within the pores after cooling. Upon filling the sample by capillary wetting, it takes approximately 1 h for the bulk of the liquid to enter the pores, as observed by the transition from transparent to opaque appearance of the sample. At this temperature, $\sim$300 K, the viscosity of MTHF is as low as $\sim 10^{-2}$ P. In the present temperature range, $T \leqslant 100$ K, the viscosity is $\eta \geqslant 10^{6}$ P, so that it is by no means trivial that constant pressure conditions are attained within the time scales of the experiment. If the liquid exchange among the pores is suppressed by the high viscosities, the pores behave like isolated volumes within the glass. In this case, the appearance of a surface layer, where the molecules are expected to be more densely packed, reduces the average particle density in the remaining pore volume with a concomitant decrease of the structural relaxation time, in accord with the experimental findings. Irrespective of the origin of the relaxation time shift, it is reasonable to attribute the confinement-induced increase of the $\alpha$-relaxation time distribution to an additional heterogeneity which stems from the site specific distance between relaxing and immobilized molecules. However, further experiments are needed to support or quantify these more speculative statements regarding the comparison between bulk and in-pore molecular dynamics.

## V. SUMMARY AND CONCLUSIONS

We have acquired solvation dynamics data for the probe molecule quinoxaline dissolved in the glass-forming liquid 2-methyltetrahydrofuran for temperatures from 80 to 100 K and in the time range 1 ms$\leqslant t \leqslant$1 s. The study compares the bulk liquid with that confined to the mesopores of sol-gel porous glasses for different pore diameters. The time-resolved Stokes shifts $\nu(t)$ or $C(t)$ observed for the porous samples not only reflect the dielectrically active structural relaxation as in the bulk system, but additionally yields direct evidence for extremely small spatial range in which the molecular dynamics couples to the solvation free energy of the chromophore. Because the total Stokes shift $\Delta\nu$ in the bulk and in the smallest pores with $\phi$=2.5 nm is practically identical, the relevant coupling range cannot exceed 2.5 nm significantly.

For the structural relaxation of the solvent we find according to Figs. 1 and 4 two relaxation processes exhibiting a pronounced separation of time scales, which differ by at least $\sim$3 orders of magnitude. On the basis of the widths of the $S_0 \leftarrow T_1$ (0-0) emission spectra, both relaxation processes are found to be active in each pore, so that the molecular dynamics appear to separate into a very slow component associated with a surface layer and a fast component assigned to the remaining inner pore liquid, which is reminiscent of the bulk $\alpha$ process. Due to their distinct dynamical behavior, the relative contributions of the two processes to the entire relaxation strength can be accurately resolved. The corresponding results compiled in Fig. 2 are consistent with a pore size independent surface layer thickness $\rho$ of $\sim$0.1 nm at the higher temperatures, and a pronounced increase of $\rho$ as the temperature is lowered until, eventually, the entire liquid in the pores participates in the surface layer dynamics at $T \approx T_g$. Accordingly, the remaining inner pore volume displaying the $\alpha$-like relaxation is subject to a strongly temperature-dependent effective pore size $\phi - 2\rho$, as indicated in Fig. 5. Relative to the bulk properties, the in-pore $\alpha$ relaxation is accelerated and related to a wider distribution of relaxation times. The impact of the effective pore size $\phi - 2\rho(T)$ on the $\alpha$ process is to gradually reduce its relaxation strength and further decrease its time scale compared to the situation where $\rho \approx 0$. Thereby, $\rho(T)$ contributes to the lowered apparent activation energy of the $\alpha$ relaxation as the pore diameter is decreased (see Fig. 3).

The features induced by geometrical confinement as summarized above are qualitatively paralleled by analogous dielectric relaxation studies which, however, are notorious to display three distinct relaxation processes.[25,30–32] In these cases, an external electric field is applied to the sample, which represents a heterogeneous dielectric material because a liquid exhibiting dc conductivity is imbibed into a dielectrically inert and insulating porous glass. Such a situation gives rise to Maxwell-Wagner polarization and thus to a loss peak in addition to those reflecting orientational polarization. The present results support this picture by revealing two processes which unambiguously stem from the orientation of permanent dipoles. Also the confinement-induced broadening and acceleration of the $\alpha$ process observed here are in qualitative accord with the findings of dielectric spectroscopy for simple liquids of low molecular weight.[25,30] The feature of a substantial change in the $\alpha$-relaxation strength with temperature is similarly found in dielectric data obtained for sol-gel-type porous glasses.[30] However, the present data is inconsistent with a straightforward relation between length scale of cooperativity and $\alpha$-relaxation strength, but argues in favor of a marked variation of the surface layer thickness $\rho$ with temperature. For Bioran-type porous glasses made by spinodal decomposition with cylindrical pores of highly defined diameter (10.2 nm$\pm$5%) no such indication exists for a variation of $\rho$ according to dielectric results for a series of low molecular weight liquids.[25] We conclude that a growing surface layer upon lowering the

temperature is characteristic only for pores with rough or fractal surfaces like in porous media obtained by sol-gel technology. A more quantitative comparison between solvation dynamics and dielectric relaxation under confinement calls for dielectric experiments on MTHF in porous glasses, which are presently not available.

As a general conclusion, we wish to emphasize that the optical technique of solvation dynamics experiments has turned out to yield complementary information with respect to dielectric spectroscopy in the context of molecular dynamics in porous media. Because a chromophore represents a highly local probe for the orientational relaxation of permanent dipoles, the ambiguity in allocating the Maxwell-Wagner process is removed. Additionally, the slower process can be identified to be active in each pore, which strongly supports the idea of a surface layer with frustrated molecular dynamics. The method of dielectric spectroscopy is bound to remain indecisive regarding this latter result.

## ACKNOWLEDGMENTS

Financial support by the Deutsche Forschungsgemeinschaft and by the Fonds der Chemischen Industrie is gratefully acknowledged. Yu.M. acknowledges financial support by the Humboldt Foundation (Germany) and the International Science Foundation (USA).

*On leave from the Institute of Macromolecular Chemistry, National Academy of Science, 253660 Kiev, Ukraine

[1] *Molecular Dynamics in Restricted Geometries*, edited by J. Klafter and J. M. Drake (Wiley, New York, 1989).
[2] J. M. Drake and J. Klafter, Phys. Today **43**, 46 (1990).
[3] W. D. Dozier, J. M. Drake, and J. Klafter, Phys. Rev. Lett. **56**, 197 (1986).
[4] R. G. Horn and J. N. Israelachvili, J. Chem. Phys. **75**, 1400 (1981).
[5] J. Van Alsten and S. Granick, Langmuir **6**, 876 (1990).
[6] G. Schwalb and F. W. Deeg, Phys. Rev. Lett. **74**, 1383 (1995).
[7] *Relaxation in Complex Systems*, edited by K. L. Ngai and G. B. Wright [J. Non-Cryst. Solids **131-133** (1991)]; *Relaxation in Complex Systems 2*, edited by K. L. Ngai, E. Riande, and G. B. Wright [J. Non-Cryst. Solids **172-174** (1994)].
[8] D. D. Awschalon and J. Warnock, Phys. Rev. B **35**, 6779 (1987).
[9] M. W. Schafer, D. D. Awschalom, J. Warnock, and G. Ruben, J. Appl. Phys. **61**, 5438 (1987).
[10] R. K. Iler, *The Chemistry of Silica* (Wiley, New York, 1979).
[11] *Dynamics of Disordered Materials*, edited by D. Richter, A. J. Dianoux, W. Petry, and J. Teixeira, Springer Proceedings in Physics Vol. 37 (Springer-Verlag, Berlin, 1989).
[12] *Disorder Effects on Relaxational Processes*, edited by R. Richert and A. Blumen (Springer-Verlag, Berlin, 1994).
[13] J. Jäckle, Rep. Prog. Phys. **49**, 171 (1986).
[14] E. Donth, *Relaxation and Thermodynamics in Polymers* (Akademie Verlag, Berlin, 1992).
[15] W. R. Ware, P. Chow, and S. K. Lee, Chem. Phys. Lett. **2**, 356 (1968).
[16] J. D. Simon, Acc. Chem. Res. **21**, 188 (1988); P. F. Barbara, *ibid.* **21**, 195 (1988).
[17] M. Maroncelli, J. Mol. Liquids **57**, 1 (1993).
[18] R. Richert, in *Disorder Effects on Relaxational Processes* (Ref. 12).
[19] R. Richert, Chem. Phys. Lett. **171**, 222 (1990).
[20] R. Richert and A. Wagener, J. Phys. Chem. **95**, 10 115 (1991).
[21] R. Richert, Chem. Phys. Lett. **199**, 355 (1992).
[22] R. Richert, F. Stickel, R. S. Fee, and M. Maroncelli, Chem. Phys. Lett. **229**, 302 (1994).
[23] A. Papazyan and M. Maroncelli, J. Chem. Phys. **95**, 9219 (1991); **102**, 2888 (1995).
[24] C. J. F. Böttcher, *Theory of Electric Polarization* (Elsevier, Amsterdam, 1973), Vol. I.
[25] J. Schüller, R. Richert, and E. W. Fischer, Phys. Rev. B **52**, 15 232 (1995).
[26] A. C. Ling and J. E. Willard, J. Phys. Chem. **72**, 1918 (1968).
[27] G. Williams and D. C. Watts, Trans. Faraday Soc. **66**, 80 (1970).
[28] D. Davidson and R. H. Cole, J. Chem. Phys. **19**, 1484 (1951).
[29] R. Richert and A. Wagener, J. Phys. Chem. **97**, 3146 (1993).
[30] M. Arndt, W. Gorbatschow, and F. Kremer (unpublished).
[31] J. Schüller, Yu. Mel'ichenko, R. Richert, and E. W. Fischer, Phys. Rev. Lett. **73**, 2224 (1994).
[32] Yu. Mel'nichenko, J. Schüller, R. Richert, B. Ewen, and C.-K. Loong, J. Chem. Phys. **103**, 2016 (1995).
[33] C. Streck and R. Richert, Ber. Bunsenges, Phys. Chem. **98**, 619 (1994).
[34] G. Adam and J. H. Gibbs, J. Chem. Phys. **43**, 139 (1965).
[35] C. L. Jackson and G. B. McKenna, J. Non-Cryst. Solids **131-133**, 221 (1991).
[36] J. Zhang, G. Liu, and J. Jonas, J. Phys. Chem. **96**, 3478 (1992).
[37] P. Pissis, D. Daoukakis-Diamanti, L. Apekis, and C. Christodoulides, J. Phys. **6**, L325 (1994).
[38] T. Ruths and A. Patkowski (private communication).